



# Enhancement on Sensitivity and Stability of Methane Sensor by Increasing Pd Amount and Acid-Assisted Loading

Yiqun Zhang<sup>1</sup>, Yingshuo Yu<sup>1</sup>, Biao Wang<sup>2</sup>, Fengmin Liu<sup>1,\*</sup>, and Geyu Lu<sup>1,\*</sup>

<sup>1</sup>State Key Laboratory on Integrated Optoelectronics, College of Electronic Science and Engineering, Jilin University, Changchun 130012, China

<sup>2</sup>Changchun Institute of Optics, Fine Mechanics and Physics, Chinese Academy of Sciences, Changchun 130033, China

(Received: 25 July 2011. Accepted: 17 December 2011)

Al<sub>2</sub>O<sub>3</sub> was loaded with different amounts (5 wt%, 10 wt%, and 15 wt%) of Pd via isometric-impregnation. Transmission electron microscopy (TEM) demonstrated that the 15 wt% Pd/Al<sub>2</sub>O<sub>3</sub> has numerous Pd nanoparticles formed on Al<sub>2</sub>O<sub>3</sub>. To decrease the hydrolysis rate of Pd(NO<sub>3</sub>)<sub>2</sub>, which could cause the formation of Pd aggregates on Al<sub>2</sub>O<sub>3</sub>, determinate concentrations of HNO<sub>3</sub> were mixed with the impregnation solution. The measuring results of TEM and Brunauer–Emmett–Teller-specific surface areas revealed that 15 wt% Pd loaded with 10 vol% HNO<sub>3</sub> has high dispersion on Al<sub>2</sub>O<sub>3</sub>. The influences of the loading amounts of Pd and the acidity of the impregnated solution on the sensitivity and stability of gas sensors were investigated. Catalytic combustion gas sensors based on 15 wt% Pd/Al<sub>2</sub>O<sub>3</sub> prepared from a 10 vol% HNO<sub>3</sub>–90 vol% Pd(NO<sub>3</sub>)<sub>2</sub> impregnating solution exhibited high responses to methane and strong ability to resist organic silicon.

**Keywords:** Pd Loading Amount, Dispersion, Acid-Assisted Loading, Methane Sensors, Stability.

## 1. INTRODUCTION

Methane (CH<sub>4</sub>) is an extremely flammable natural gas that has wide industrial and domestic applications. A CH<sub>4</sub> leak may result in violent explosions and fire. Therefore, highly sensitive and stable CH<sub>4</sub> sensors are urgently needed. To date, catalytic combustion CH<sub>4</sub> (CCM) sensors are widely used in homes and coal mines because of their simple structure, low cost, high sensitivity, and good stability. Pd/Al<sub>2</sub>O<sub>3</sub> is recognized as the most active catalyst for the combustion of CH<sub>4</sub>.<sup>1–3</sup> However, this catalyst suffers from deactivation problems mainly due to large Pd aggregations on Al<sub>2</sub>O<sub>3</sub> that occur during combustion. Previous studies have found that the response of a Wheatstone bridge-based CCM sensor using Pd/Al<sub>2</sub>O<sub>3</sub> to 10000 ppm methane is lower than 30 mV.<sup>4–6</sup> Although the effects of particle size,<sup>7–9</sup> Pd species,<sup>10</sup> and surface state of the support<sup>1,11</sup> on the sensing performance have already been reported, few studies have focused on the effect of Pd dispersion<sup>12–15</sup> on catalyst deactivation in CH<sub>4</sub> combustion. The effect of the acidity of the impregnated solution

on the Pd catalyst morphology and sensing performance has also been rarely studied.

Pd/Al<sub>2</sub>O<sub>3</sub> catalyst is usually prepared by first forming Al<sub>2</sub>O<sub>3</sub> powder via a precipitation-and-calcination process. Fine Pd-containing compounds are then impregnated into the Al<sub>2</sub>O<sub>3</sub> particles. Several loading methods have been developed, such as precipitate deposition,<sup>13</sup> wet impregnation,<sup>16</sup> and ultrasonic impregnation.<sup>17</sup> Among these methods, isometric impregnation<sup>18–22</sup> is the most extensively used because of its simple operation, low cost, high utilization ratio, and good repeatability. The loading process comprises the transport of Pd<sup>2+</sup> into Al<sub>2</sub>O<sub>3</sub>, and the hydrolysis of Pd<sup>2+</sup> on Al<sub>2</sub>O<sub>3</sub>. If the hydrolysis rate of Pd(NO<sub>3</sub>)<sub>2</sub> is fast, Pd will aggregate on Al<sub>2</sub>O<sub>3</sub>. Hence, decreasing the hydrolysis rate of Pd(NO<sub>3</sub>)<sub>2</sub> is very important to obtain highly dispersed Pd catalyst.

In the present work, the Pd loading amount was increased from 5 wt% to 15 wt% to retain Pd activity during combustion. Nitric acid was also added to the impregnated solution to improve the dispersion of Pd. The effects of the loading amount and the acidity of the impregnated solution on the morphology and dispersion of Pd on Al<sub>2</sub>O<sub>3</sub>

\*Corresponding authors; Emails: liufm@jlu.edu.cn; luyg@jlu.edu.cn

were investigated. The corresponding sensing properties and stability of the CCM sensors were also examined.

## 2. EXPERIMENTAL METHODS

### 2.1. Preparation of Al<sub>2</sub>O<sub>3</sub> Support and Loading of Pd Catalyst

Al<sub>2</sub>O<sub>3</sub> was prepared by sintering commercial Al<sub>2</sub>O<sub>3</sub> · H<sub>2</sub>O (321-25785 Boehmite, Wako) at 750 °C for 6 h. The noble metal Pd was loaded on the as-prepared Al<sub>2</sub>O<sub>3</sub> using isometric impregnation. For this impregnation, the maximum volume of Pd(NO<sub>3</sub>)<sub>2</sub> solution that can be absorbed by Al<sub>2</sub>O<sub>3</sub> powder was mixed with Al<sub>2</sub>O<sub>3</sub> at room temperature. The mixture was then steeped for 2 h. The loading amount and HNO<sub>3</sub> concentration in the impregnation solution were both adjusted. Finally, the precursors of Pd/Al<sub>2</sub>O<sub>3</sub> prepared with these loading conditions were dried at 80 °C for 1 h. Reduction under a mixed atmosphere of 5% H<sub>2</sub> in N<sub>2</sub> followed at 290 °C for 2 h.

### 2.2. Characterization of Pd/Al<sub>2</sub>O<sub>3</sub>

X-ray diffraction (XRD, Rigaku wide-angle X-ray diffraction D/max rA, using Cu K $\alpha$  radiation at wavelength  $\lambda = 0.1541$  nm) was carried out to examine the structure of Pd catalyst. The Brunauer–Emmett–Teller (BET)-specific surface areas of the samples were measured by nitrogen adsorption measurements (Gemini VII 2390). The as-reduced Pd/Al<sub>2</sub>O<sub>3</sub> materials with different loading conditions were further characterized by transmission electron microscopy (TEM, HITACHI H-8100) to determine the morphology and dispersion of Pd on Al<sub>2</sub>O<sub>3</sub>.

### 2.3. Fabrication and Measurement of the Sensors

The sensing and reference elements were fabricated by coating the obtained Pd/Al<sub>2</sub>O<sub>3</sub> and pure Al<sub>2</sub>O<sub>3</sub> with a soft brush under the control of a digital viewer (GE-5), respectively, onto platinum coils, and then sintered at 600 °C for 2 h. The obtained two elements were connected in series with each other in a Wheatstone bridge.<sup>5</sup> In order to keep the sensing and reference devices at 450 °C in air, 2.5 V of voltage was applied between the two devices. When the sensor was exposed to methane, the temperature of the sensor increased, because the combustion heat would be transferred to the sensing element. The temperature of sensor can be extracted by the following well known equation:<sup>23</sup>

$$T = T_0 + (R - R_0)/R_0 * \alpha \quad (1)$$

The response is the difference of the outputs in air and methane.

The invalidation of methane sensors mainly result from the adsorption of organic silicon while the methane sensors work in coal mine or kitchen. Hence, to examine the

stability of the methane sensors in the present study, 2 g of organic silicon was placed in a 50 L airtight box and the methane sensors were heated by the Joule heat of the Pt coils in the box. The silicon source was replaced a day once, and the sensitivities of the methane sensors under the durability were tested until 34 days.

## 3. RESULTS AND DISCUSSION

### 3.1. Characterization of Pd/Al<sub>2</sub>O<sub>3</sub>

The XRD patterns of 5, 10 and 15 wt% Pd/Al<sub>2</sub>O<sub>3</sub> catalysts obtained by isometric impregnation are shown in Figure 1, and those of 15 wt% Pd/Al<sub>2</sub>O<sub>3</sub> catalysts prepared from the impregnation solution containing different HNO<sub>3</sub> concentrations (4 vol%, 10 vol%, and 25 vol%) are displayed in Figure 2. The results indicated that pure metal Pd was formed on the surface of Al<sub>2</sub>O<sub>3</sub> support. The Pd grain sizes of these samples are further calculated using Scherrer equation, shown in Table I.

The BET-specific surface areas of the as-prepared samples are shown in Table II. The specific surface areas decreased with the increasing of Pd loading amount because more Al<sub>2</sub>O<sub>3</sub> surfaces were covered. On the other hand, the specific surface areas evidently increased with the increasing of HNO<sub>3</sub> concentration when the HNO<sub>3</sub>

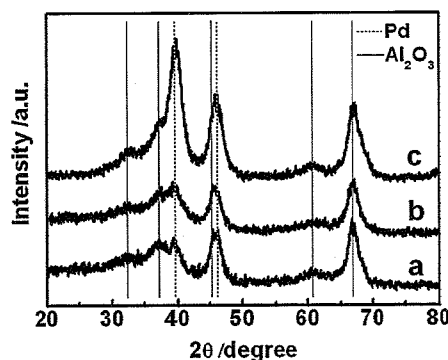


Fig. 1. XRD pattern of Pd/Al<sub>2</sub>O<sub>3</sub> versus (a) 5 wt%, (b) 10 wt%, and (c) 15 wt% Pd loading amount.

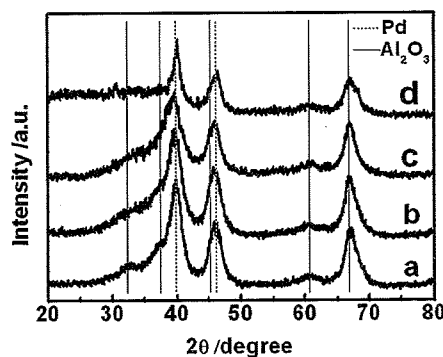
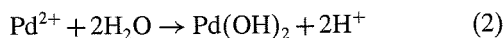


Fig. 2. XRD pattern of Pd/Al<sub>2</sub>O<sub>3</sub> versus (a) 0 vol%, (b) 4 vol%, (c) 10 vol%, and (d) 25 vol% HNO<sub>3</sub> concentration.

**Table I.** Pd grain size of Pd/Al<sub>2</sub>O<sub>3</sub> obtained under different conditions.

Loading amount	Pd grain size (nm)
Pd	
5 wt% Pd	8.67
10 wt% Pd	8.49
15 wt% Pd	8.75
HNO <sub>3</sub>	
0 vol%	8.75
4 vol%	8.51
10 vol%	8.39
25 vol%	12.86

concentration was lower than 10 vol%. This result was due to the decreasing of Pd<sup>2+</sup> hydrolysis rate induced by adding HNO<sub>3</sub>. The reaction formula of the Pd<sup>2+</sup> hydrolysis process could be expressed as following:



H<sup>+</sup> concentration was increased with HNO<sub>3</sub> adding, which inhibit the reaction of Eq. (2), so the hydrolysis rate of Pd<sup>2+</sup> was reduced. However, when the HNO<sub>3</sub> concentration was 25 vol%, the specific surface areas suddenly decreased probably because of the corrosion of Al<sub>2</sub>O<sub>3</sub>.

Figure 3 shows the TEM images and corresponding Pd particle size distributions of the Pd/Al<sub>2</sub>O<sub>3</sub> catalysts with different Pd loading amounts (5 wt%, 10 wt%, and 15 wt%) as well as from the impregnation solution containing different HNO<sub>3</sub> concentrations. From the TEM images, it can be seen that the Pd particles (black color in TEM) were formed on the surface of in all these cases, and the amount of Pd on Al<sub>2</sub>O<sub>3</sub> support increased with the increasing of Pd loading amount (Figs. 3(a–c)). The corresponding Pd size are relatively uniform, about 8 nm, and Pd size distributions are shown in Figures 3(a'–c'), which are consistent with the average grain size estimated from the XRD analysis. The 15 wt% Pd/Al<sub>2</sub>O<sub>3</sub> obviously had numerous Pd catalysts on Al<sub>2</sub>O<sub>3</sub>, and was expected to show the highest response, compared with the 5 wt% and 10 wt% Pd /Al<sub>2</sub>O<sub>3</sub>. The size uniformity of Pd particles on Al<sub>2</sub>O<sub>3</sub> was also evidently improved by

increasing HNO<sub>3</sub> concentration (Figs. 3(d–f, d'–f')). However, when the HNO<sub>3</sub> concentration was 25 vol%, large Pd aggregations appeared on Al<sub>2</sub>O<sub>3</sub> and the size of Pd catalyst was enlarged from 8 nm to 10 nm. The relationship of Pd formation pathways and HNO<sub>3</sub> concentrations were shown in Figure 4. The hydrolysis rate of Pd<sup>2+</sup> on Al<sub>2</sub>O<sub>3</sub> was restricted to a certain extent when the acidity of the impregnated solution was sufficient, consequently, the Pd size uniformity was improved, which were shown in Figures 4(a and b). When the HNO<sub>3</sub> concentration was excess, the Al<sub>2</sub>O<sub>3</sub> structure was destroyed which cause many Pd particles aggregated on Al<sub>2</sub>O<sub>3</sub> shown in Figure 4(c). Therefore, the catalyst with 15 wt% Pd/Al<sub>2</sub>O<sub>3</sub> obtained from the impregnated solution containing 10 vol% HNO<sub>3</sub> showed the highest response among all samples.

### 3.2. Methane-Sensing Properties of Pd/Al<sub>2</sub>O<sub>3</sub>

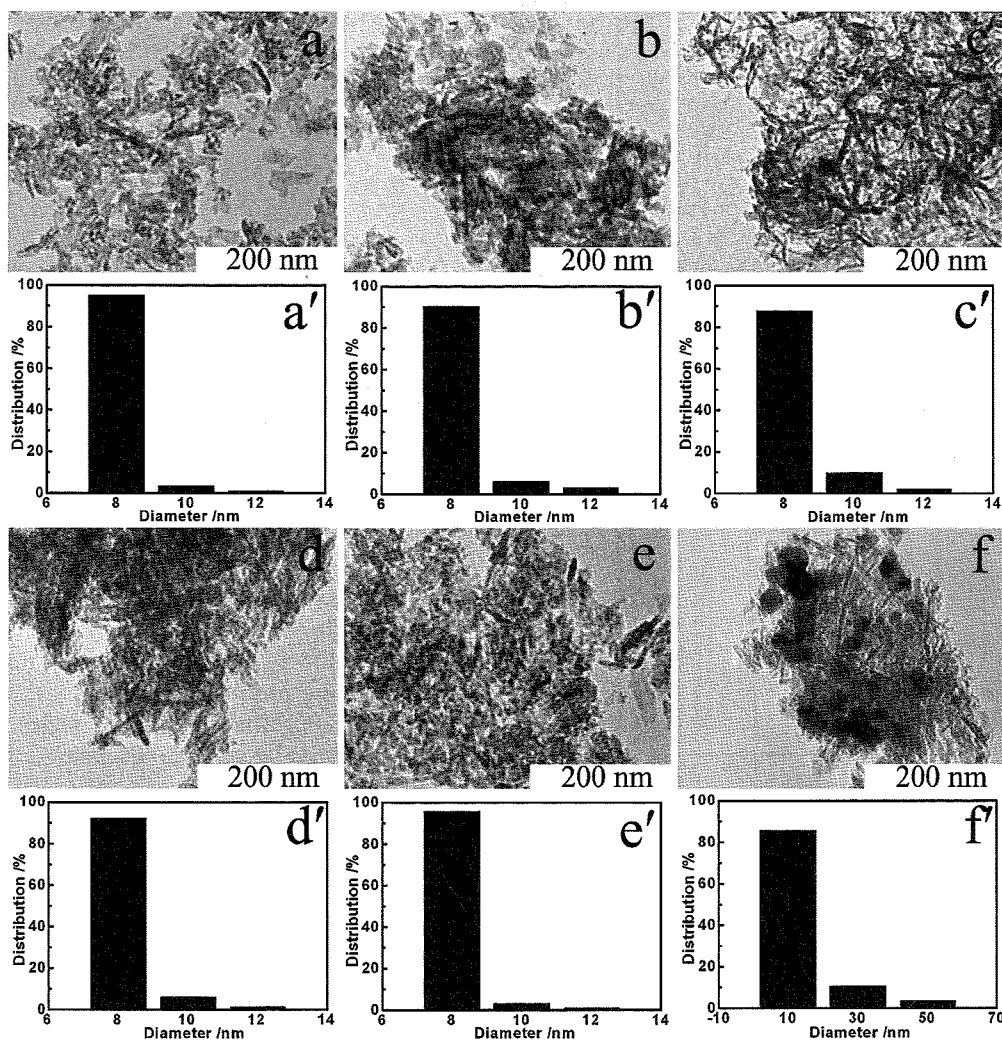
Figure 5 shows the methane-sensing properties of catalytic combustion sensors based on Pd/Al<sub>2</sub>O<sub>3</sub> material with different Pd loading amounts. The response of the sensor to 10000 ppm methane was improved from 24.7 mV to 34.1 mV when the Pd loading amount was increased from 5 wt% to 15 wt%. This result is attributed to the increased oxidation activity to CH<sub>4</sub> and of the improved heat conductivity. These results showed that the loading amount significantly influences Pd dispersion and the methane-sensing property of Pd/Al<sub>2</sub>O<sub>3</sub>.

Figure 6 shows the response of the methane sensors based on 15%wt Pd/Al<sub>2</sub>O<sub>3</sub> material obtained from impregnated solution containing various HNO<sub>3</sub> concentrations. The response of the methane sensor to 10000 ppm methane was enhanced from 34.1 mV to 37.7 mV when the HNO<sub>3</sub> concentration was increased from 0 vol% to 10 vol%. Pd dispersion also apparently improved. However, the response of the methane sensor decreased to 30.1 mV when the HNO<sub>3</sub> concentration was increased to 25 vol%. This is because some large Pd aggregations were formed on Al<sub>2</sub>O<sub>3</sub>. These findings illustrated that the response of Pd/Al<sub>2</sub>O<sub>3</sub> was closely related to the acidity of the impregnated solution and the dispersion of Pd.

The response and recovery curves of the catalytic combustion sensors based on Pd/Al<sub>2</sub>O<sub>3</sub> material with different Pd loading amounts (5 wt%, 10 wt%, and 15 wt%) to 2000 ppm CH<sub>4</sub> are shown in Figures 7(a–c), respectively. All the sensors using different Pd loading amounts on Al<sub>2</sub>O<sub>3</sub> catalysts display quick response and recovery speeds to methane, the response is about 4 s and the recovery time is about 7 s, however, the repeatability is obviously different. The outputs both in air and 2000 ppm methane for the sensors based on 5 wt%, 10 wt% Pd/Al<sub>2</sub>O<sub>3</sub> are upwards after three cycles. At the same time, Figure 7(c) showed that the outputs in air and 2000 ppm methane are repeatable for the sensors using 15 wt% Pd/Al<sub>2</sub>O<sub>3</sub>. Figure 8

**Table II.** BET-specific surface areas of Pd/Al<sub>2</sub>O<sub>3</sub> obtained under different conditions.

Loading amount	Specific surface area (m <sup>2</sup> · g <sup>-1</sup> )
Pd	
5 wt% Pd	187.2
10 wt% Pd	179.4
15 wt% Pd	175.1
HNO <sub>3</sub>	
0 vol%	175.1
4 vol%	180.6
10 vol%	180.3
25 vol%	174.0



**Fig. 3.** TEM images of Pd/Al<sub>2</sub>O<sub>3</sub> versus (a) 5 wt%, (b) 10 wt%, and (c) 15 wt% Pd loading amount and (d) 4 vol%, (e) 10 vol%, and (f) 25 vol% HNO<sub>3</sub> concentration and the corresponding Pd size distribution of Pd/Al<sub>2</sub>O<sub>3</sub> (a'–f')

shows the response and recovery curves of the methane sensors versus HNO<sub>3</sub> concentration. There are some output drifts in air after three cycles for the sensors using 15 wt% Pd/Al<sub>2</sub>O<sub>3</sub> with various HNO<sub>3</sub> concentrations. In addition, the sensor using 15 wt% Pd/Al<sub>2</sub>O<sub>3</sub> impregnated by 10 vol% HNO<sub>3</sub> solution shows a repeatable response to

2000 ppm methane. Above results indicated that Pd loading amounts and the acidity of the impregnating solution haven't evident influence to the response and recovery except repeatability of the methane sensors.

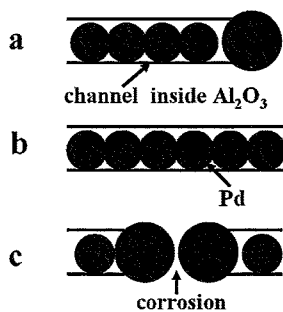


**Fig. 4.** Pd formation pathways versus various HNO<sub>3</sub> concentrations, scarcity (a), sufficiency (b) and excess (c).

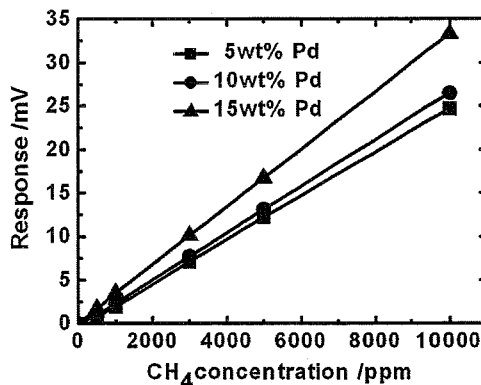


**Fig. 5.** Response of the sensors versus the Pd loading amount.

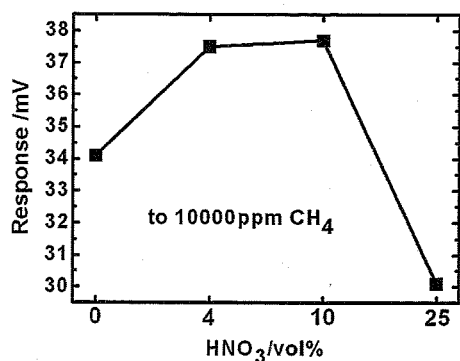


Fig. 6. Response of the sensors versus  $\text{HNO}_3$  concentration.

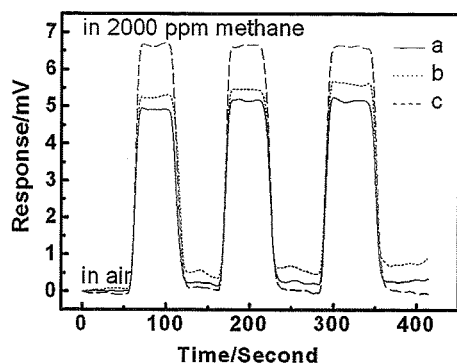


Fig. 7. The response and recovery curves of the sensors versus Pd loading amount ((a) 5 wt%, (b) 10 wt%, and (c) 15 wt%).

### 3.3. Stability of the Sensors

Figure 9 shows the long-term stabilities of the methane sensors under organic silicon atmosphere. The sensitivity ratio was defined as the ratio of the degraded ( $R$ ) and initial ( $R_0$ ) Responses. Organic silicon greatly affected the sensitivity because it was adsorbed on the surface of the Pd catalyst in the organic silicon atmosphere, transformed into  $\text{SiO}_2$  at elevated temperature, and then covered the Pd catalyst in high temperatures. The resistance of  $\text{Pd}/\text{Al}_2\text{O}_3$  against organic silicon was improved by increasing Pd loading amount. The response ratios after 34 days

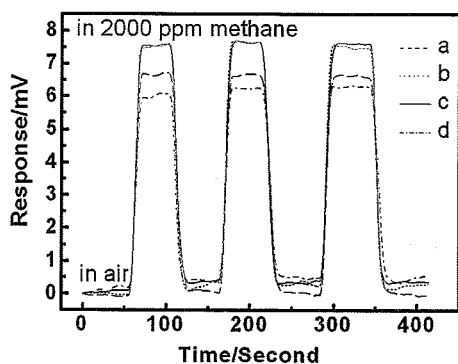


Fig. 8. The response and recovery curves of the sensors versus  $\text{HNO}_3$  concentration ((a) 0 vol%, (b) 4 vol%, (c) 10 vol%, and (d) 25 vol%).

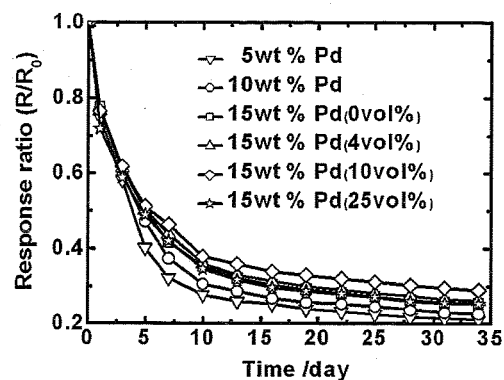


Fig. 9. Response ratios of the sensors under various loading conditions.

were 0.21, 0.22, and 0.25, corresponding to the Pd loading amounts of 5 wt%, 10 wt%, and 15 wt%, respectively. Compared with 15 wt%  $\text{Pd}/\text{Al}_2\text{O}_3$ , the amount of Pd catalyst was less in 5 wt%  $\text{Pd}/\text{Al}_2\text{O}_3$  and 10 wt%  $\text{Pd}/\text{Al}_2\text{O}_3$ , thereby accelerating the aging speed. The response ratio of the sensor improved to 0.29 when the  $\text{HNO}_3$  concentration increased to 10 vol%. These results further illustrated that the stability of the sensors was closely related to the dispersion of Pd. The most stable sensor was based on 15 wt%  $\text{Pd}/\text{Al}_2\text{O}_3$  materials obtained from impregnation with 10 vol%  $\text{HNO}_3$ .

## 4. CONCLUSIONS

Different Pd loading amounts and the acidity of the impregnating solution resulted in varying levels of Pd dispersion. Consequently, the sensing properties and stability of a CCM sensor were affected. The 15 wt%  $\text{Pd}/\text{Al}_2\text{O}_3$ -based sensor had the highest sensing properties and stability among the three Pd loading amounts. Pd dispersion was improved when the hydrolysis rate of  $\text{Pd}(\text{NO}_3)_2$  was restricted to 10 vol%  $\text{HNO}_3$  in a  $\text{Pd}(\text{NO}_3)_2$  impregnation solution. Increasing the loading amount and dispersion of Pd on  $\text{Al}_2\text{O}_3$  can enhance the sensitivity and stability of methane sensors using  $\text{Pd}/\text{Al}_2\text{O}_3$ .

**Acknowledgments:** This work was supported by the National Science Fund (No. 60906036, No. 61074172).

## References and Notes

1. P. Gelin and M. Primet, *Appl. Catal. B: Environ.* 39, 1 (2002).
2. D. L. Mowery, M. S. Graboski, T. R. Ohno, and R. L. McCormick, *Appl. Catal. B: Environ.* 21, 157 (1999).
3. D. L. Mowery and R. L. McCormick, *Appl. Catal. B: Environ.* 34, 287 (2001).
4. P. T. Moseley, *Meas. Sci. Technol.* 8, 223 (1997).
5. Y. Wang, M. M. Tong, D. Zhang, and Z. Gao, *Sensors* 11, 19 (2011).
6. X. W. Ren, Z. Z. Xu, and B. Zhou, *Transducer and Microsystem Technologie* 28, 30 (2009).
7. C. A. Müller, M. Maciejewski, R. A. Koeppel, and Á. Baiker, *J. Catal.* 166, 36 (1997).
8. R. F. Hicks, H. Qi, M. L. Young, and R. G. Lee, *J. Catal.* 122, 280 (1990).

9. C. A. Muller, M. Maciejewski, R. A. Koeppe, and A. Baiker, *Catal. Today* 47, 245 (1999).
10. J. Vinod Kumar, N. Lingaiah, K. S. Rama Rao, S. P. Ramnani, S. Sabharwal, and P. S. Sai Prasad, *Catal. Commun.* 10, 1149 (2009).
11. D. Ciuparu, M. R. Lyubovsky, E. Altman, L. D. Pfefferle, and A. Datye, *Catal. Rev.: Sci. Eng.* 44, 593 (2002).
12. C. He, P. Li, H. L. Wang, J. Cheng, X. Y. Zhang, and Y. F. Wang, *J. Hazard. Mater.* 181, 996 (2010).
13. S. D. Oh, B. K. So, S. H. Choi, A. Gopalan, K. P. Lee, K. R. Yoon, and I. S. Choi, *Mater. Lett.* 59, 1121 (2005).
14. V. I. Zarko, V. M. Gun'ko, L. S. Andriyko, E. V. Goncharuk, M. Matysek, and E. Skwarek, *Surf. Chem. Biomed. Environ. Sci.* 429 (2006).
15. I. E. Beck, V. V. Kriventsov, B. N. Novgorodov, E. P. Yakimchuk, D. I. Kochubey, and V. I. Zaikovskiy, *Nucl. Instrum. Meth. A* 603, 178 (2009).
16. M. Chen, L. Y. Qi, L. P. Fan, R. X. Zhou, and X. M. Zheng, *Mater. Lett.* 62, 3646 (2008).
17. C. L. Bianchi, E. Gotti, L. Toscano, and V. Ragaini, *Ultrason. Sonochem.* 4, 317 (1997).
18. J. S. Zhang, W. L. Luan, H. Huang, Y. S. Qi, and S. T. Tu, *Sens. Actuators B: Chem.* 128, 266 (2007).
19. D. M. Luo, Y. Bi, W. Kan, N. Zhang, and S. G. Hong, *J. Mol. Struct.* 994, 325 (2011).
20. L. L. Kong, S. H. Zhong, Y. Liu, and X. F. Xiao, *Acta Chim. Sinica.* 64, 409 (2006), in Chinese.
21. L. L. Kong, S. H. Zhong, and Y. Liu, *Chinese J. Catal.* 26, 917 (2005), in Chinese.
22. Q. Zhang, H. F. Wang, G. S. Sun, K. L. Huang, W. P. Fang, and Y. Q. Yang, *Chinese J. Inorg. Chem.* 25, 1384 (2009), in Chinese.
23. L. Xu, T. Li, X. L. Gao, and Y. L. Wang, *IEEE Sensors* 391 (2010).